

# Calibration of the transient field for Pt ions in gadolinium and magnetic moments of the $2_1^+$ states in $^{196,198}\text{Pt}$

R. Tanczyn

*Department of Physical Science, Kutztown University, Kutztown, Pennsylvania 19530*

G. Kumbartzki, A. Piqué,\* T. Vass, A. Pakou,† and N. Benczer-Koller

*Department of Physics and Astronomy, Rutgers University, New Brunswick, New Jersey 08903*

(Received 7 October 1992)

The precession of the angular distribution of gamma rays deexciting the  $2_1^+$  states of  $^{194,196,198}\text{Pt}$  and  $^{148}\text{Nd}$  nuclei have been measured by the transient field method. Average values of the transient field acting at Pt and Nd ions recoiling through gadolinium have been obtained from these data, and are shown to validate the Rutgers parametrization in the recoil velocity range  $1.9 \leq (v/v_0) \leq 4.6$ . The  $g(2_1^+)$  factors of  $^{196,198}\text{Pt}$  relative to  $g(^{194}\text{Pt}) = 0.302(16)$  have also been deduced:  $g(^{196}\text{Pt}) = 0.302(24)$  and  $g(^{198}\text{Pt}) = 0.350(30)$ , in good agreement with other transient field measurements.

PACS number(s): 21.10.Ky

## I. INTRODUCTION

The discovery [1] of large magnetic fields that act on ions as they travel through iron, cobalt, nickel, and gadolinium has led to the development of techniques [2, 3] for the measurement of magnetic moments of short-lived excited nuclear states. These techniques employ the detection of the hyperfine interaction between the electronic environment and the nuclear moments of excited nuclei as they traverse thin polarized ferromagnetic foils. The angular precession of the magnetic moment in this effective transient field is proportional to both the moment, or  $g$  factor, and the magnetic field. If either the excited-state  $g$  factor or the transient field (TF) is known, the other can be extracted from a measurement of the precession of the decay gamma-ray angular correlation. Attempts to parametrize the transient field as a function of atomic number and recoil velocity by a single expression [4–7] have met with some success, particularly in the intermediate mass region. Measurements to determine the transient field acting at heavier ions ( $Z \geq 70$ ) through  $g$ -factor measurements have, however, produced inconsistent results.

Measurements by the Rutgers group [8] on  $^{186,188}\text{Os}$  and  $^{194,196}\text{Pt}$  recoiling through magnetized iron yielded  $g$  factors for the  $2_1^+$  states in Os in agreement with those obtained by Mössbauer experiments, essentially verifying the Rutgers calibration [6] of the transient field. Although there was no reason to assume a dramatic variation of the transient field with  $Z$  between Os and Pt, the  $g$  factors deduced from the parametrization for the  $2_1^+$

states in  $^{194,196}\text{Pt}$  were found to be  $\approx 30\%$  smaller (approximately 0.2) than those determined by radioactivity or ion implantation methods (approximately 0.3).

A transient field experiment by the Australian group [9] on  $^{192}\text{Os}$  and  $^{198}\text{Pt}$  recoiling through magnetized cobalt foils yielded precession data in agreement with the Rutgers result, but led to an interpretation of the transient hyperfine field in contradiction with the Rutgers calibration. This group concluded that the transient field acting on Pt in cobalt is the same as the field acting on Os, but for recoil through iron, the field acting on Pt is much smaller than the corresponding field acting on Os. These investigators suggested that the overlap of the  $4s$  and  $2p$  electron energy levels was different in Pt/iron than in Os/iron, corresponding to a smaller transient field at Pt nuclei recoiling in iron than at Os nuclei. A similar energy level match for Os in iron or for Pt and Os in cobalt does not exist; hence, a transient field as predicted by the Rutgers parametrization for these ion/host pairs was observed [9].

Other contradictions were noted in an experiment on  $^{197}\text{Au}$ ,  $^{194,196}\text{Pt}$ , and  $^{184,186}\text{W}$  recoiling in gadolinium performed at Legnaro by a Padova collaboration [10]. The precessions measured in that work, in which the higher ( $\approx 0.3$ )  $g$  factor was taken as an adopted value for the excited Pt nuclei, were in agreement with the predictions of the Chalk River parametrization [11] of a higher field in gadolinium than in iron. Further, the Padova group concluded that the transient field in iron is anomalously low for Pt, but that no such anomaly occurs for Au or W.

The inconsistencies in the results of the transient field experiments is indicative of the risk involved in the application of the field parametrizations in the determination of  $g$  factors. Since it is reasonable to expect that the transient field should rely on the magnetization of the ferromagnetic host as well as on  $Z$  and the velocity of the recoiling ion, precise knowledge of the physical and kine-

\*Present address: NEOCERA, 335 Paint Branch Drive, College Park, MD 02742.

†Present address: Department of Physics, University of Ioannina, Ioannina, Greece.

matic properties of the targets used is essential. Further potential problems may also arise from beam-induced attenuations of the transient field as reported by Speidel *et al.* [12, 13].

These difficulties can be circumvented by the measurement of the precession of a known magnetic moment in the same recoiling nucleus or in another isotope of the same nucleus. Unfortunately, there is no excited state in a Pt isotope whose magnetic moment is unambiguously known. A second approach involves the simultaneous measurement of the precession of the gamma-ray angular distribution of transitions in neighboring nuclei and the use of more than one ferromagnetic host to avoid the pitfall discussed above. Such a calibration was employed by the Australian group [14] in which the precessions in  $^{194,196,198}\text{Pt}$  ( $Z = 78$ ) recoiling in gadolinium were measured simultaneously with those of  $^{182,184,186}\text{W}$  ( $Z = 74$ ). These measurements resulted in  $g$  factors for the  $2_1^+$  states in Pt of  $\approx 0.3$ . Further evidence of the larger  $2_1^+$   $g$  factors arises from a recent transient field experiment on  $^{192,194,196}\text{Pt}$  recoiling in iron and gadolinium at Legnaro [15] and by a high precision integral perturbed angular correlation (IPAC) measurement using the static hyperfine field acting at  $^{192}\text{Pt}$  in iron [16]. This latter measurement by Bodenstedt *et al.* resulted in a value for the static field in excellent agreement with that determined by Kontani and Itoh [17] and confirmed the reliability of the  $g$ -factor results for  $^{192,194}\text{Pt}$  of Katayama, Morinobu, and Ikegama [18] determined by radioactivity methods. These measurements all support an anomalously low transient field for Pt in iron.

The Rutgers parametrization of the transient field has been previously established for excited ions recoiling through iron. After the shutdown of the Rutgers Tandem, experiments were continued at Yale University. The heavier ion beams and higher beam energies available at Yale provided the opportunity and the need to reevaluate the Rutgers parametrization. The purpose of the work reported in this paper has been to extend the calibration to heavier nuclei recoiling at higher velocities through gadolinium. The value  $g = 0.302(16)$  was adopted for the  $2_1^+$  state in  $^{194}\text{Pt}$  from the radioactivity measurement (IPAC in iron) of Katayama, Morinobu, and Ikegama recalculated to include a new life-

time determination  $\tau = 59.7(22)$  ps [19]. The gamma-ray angular precessions for the three  $2_1^+ \rightarrow 0_1^+$  transitions in  $^{194,196,198}\text{Pt}$  produced by recoil through magnetized gadolinium were measured simultaneously. Average values for the transient field were calculated from the precessions and the  $g$  factors for the  $2_1^+$  states in  $^{196,198}\text{Pt}$  calculated relative to that of  $^{194}\text{Pt}$ .

## II. EXPERIMENT

Experiments employing the transient field technique are designed to detect the precession of the excited-state magnetic moment about the direction of the transient magnetic field. The precession is determined by measuring the rotation of the gamma-ray angular correlation from the traversal of the excited ions through a thin polarized ferromagnetic foil. These experiments have been described in many publications [20, 21]; experimental details unique to this work will be outlined here.

The work reported here was conducted at the Nuclear Physics Laboratory of Rutgers University and at the A. W. Wright Nuclear Structure Laboratory of Yale University. At Rutgers, beams of 77 MeV  $^{32}\text{S}^{9+}$  ions from the Rutgers FN-Tandem accelerator were used to Coulomb-excite the  $2_1^+$  states in  $^{194}\text{Pt}$  ( $E_\gamma = 0.328$  MeV),  $^{196}\text{Pt}$  ( $E_\gamma = 0.356$  MeV), and  $^{198}\text{Pt}$  ( $E_\gamma = 0.407$  MeV). At Yale University, beams of 80 MeV  $^{32}\text{S}^{9+}$  and 150 MeV  $^{58}\text{Ni}^{11+}$  ions from the Yale ESTU-Tandem accelerator were used to produce the excitation. The more energetic beams available from the Yale ESTU allowed the study of higher recoil velocities and provided higher gamma-ray yields from enhanced reaction cross section and thicker targets.

Three different multilayer targets, whose structure is given in Table I, were used in four runs. Runs II and III were performed on the same target which provided overlapping recoil velocities to runs I and IV. Recoil energies shown in the table were calculated using Ziegler stopping powers [22]. The Pt layer for each target was produced by electroplating. Separate solutions of  $^{194}\text{Pt}$  (95.1% enriched),  $^{196}\text{Pt}$  (97.5%), and  $^{198}\text{Pt}$  (95.8%) were prepared by first dissolving the separated isotope in Aqua Regia and then evaporating the liquid over a 2

TABLE I. Summary of target structure and kinematics of the recoiling Pt ions.  $l$  is the thickness of the  $^{194,196,198}\text{Pt}$  layer and  $L$  the thickness of the gadolinium foil.  $M$  is the target magnetization in tesla measured at 40 K.  $E_{\text{in}}$  and  $E_{\text{out}}$  are the average energies based on stopping powers tabulated by Ziegler [22] for Pt ions traversing the gadolinium.  $\langle v/v_0 \rangle$  is the average ion velocity in units of the Bohr velocity  $v_0 = e^2/\hbar$ . Runs II and III were performed with the same target.

Run	Beam	$l$ (mg/cm <sup>2</sup> )	$L$ (mg/cm <sup>2</sup> )	$M$ (T)	$E_{\text{in}}$ (MeV)	$E_{\text{out}}$ (MeV)	$\langle \frac{v}{v_0} \rangle_{\text{in}}$	$\langle \frac{v}{v_0} \rangle_{\text{out}}$
I	77 MeV $^{32}\text{S}$	0.550 <sup>a</sup>	1.96	0.1230	33.44	17.47	2.63	1.91
II	80 MeV $^{32}\text{S}$	0.367	2.29	0.1740	36.43	17.08	2.75	1.88
III	150 MeV $^{58}\text{Ni}$	0.367	2.29	0.1740	102.62	58.20	4.59	3.50
IV	150 MeV $^{58}\text{Ni}$	0.622 <sup>b</sup>	3.23	0.1580	97.85	40.95	4.51	2.92

<sup>a</sup>Pt layer covered by 0.185 mg/cm<sup>2</sup>  $^{148}\text{Nd}$ .

<sup>b</sup>Pt layer covered by 0.215 mg/cm<sup>2</sup>  $^{148}\text{Nd}$ .

day period by gentle heating. Plating solutions of each isotope were produced by adding a buffer solution of  $\text{Na}_2\text{HPO}_4 + 12\text{H}_2\text{O}$  and  $(\text{NH}_4)_2\text{PO}_4$  (5.3:1 ratio) to the residue. The buffered solutions were warmed for approximately 12 h until clear and then combined to form a composite solution of 24%  $^{194}\text{Pt}$ , 29%  $^{196}\text{Pt}$ , and 47%  $^{198}\text{Pt}$ . The composite solution was plated onto natural gadolinium foil which had been rolled and later annealed under a  $10^{-6}$  Torr vacuum by resistance heating. A backing layer of copper thick enough to stop the recoiling Pt ions was evaporated on the opposite side of the gadolinium. The targets used in two of the four runs indicated in Table I were covered with an additional thin layer of  $^{148}\text{Nd}$  evaporated on the Pt surface. The intended purpose of this layer was to measure the angular precessions in the Pt relative to that of the  $2_1^+ \rightarrow 0_1^+$  transition in  $^{148}\text{Nd}$  and, in a separate experiment, to that of the  $2_1^+ \rightarrow 0_1^+$  transition in  $^{188}\text{Os}$  from a  $^{148}\text{Nd}/^{188}\text{Os}$  target. Thus the  $g$  factors of Pt would have been calibrated against the well-established  $2_1^+$   $g$  factor of the neighboring ( $Z = 76$ )  $^{188}\text{Os}$  with the  $^{148}\text{Nd}$  transition acting as an intermediate reference. While this goal was sound in principle, it produced unsatisfactory results due to the mathematical propagation of the statistical experimental errors. The 0.302 MeV gamma rays from  $^{148}\text{Nd}$  did not interfere with the measurements for Pt. The Nd did, however, provide a means to check the magnetic quality of the gadolinium layer. The measured precession and the calculated transient field acting on Nd have been included in the results.

The choice of gadolinium over iron for the ferromagnetic layer takes advantage of the generally lower stopping power for heavy ions in gadolinium. This characteristic allows for a thicker ferromagnetic layer and for a subsequently longer time of interaction between the nuclear moment and the transient field. However, since the Curie temperature for gadolinium is 295 K, it is necessary to cool the targets in order to saturate the target magnetization and to maximize the rotation of the moment. A precise determination of the target magnetization is essential for the application of a transient field parametrization in the measurement of  $g$  factors. A measurement by the Rutgers group [23] of the precession of the  $^{150}\text{Sm}$   $2_1^+$  moment in gadolinium as a function of temperature and target magnetization is shown in Fig. 1. The figure clearly indicates that the hyperfine interaction closely follows the magnetization curve. The magnetization of each target in a polarizing field of 0.09 T was measured as a function of temperature before and after each run using a low temperature ac magnetometer [24]. The results of these measurements are shown in Fig. 2. As the figure indicates, the magnetization of all targets was fairly constant over a temperature range of 40–100 K. However, the plots indicate large variations in magnetization that arise with temperature in any one particular foil and in the overall magnetization of separate foils. As shown in Ref. [24], the magnetization of thin gadolinium foils can vary greatly with temperature, polarizing field, and thickness. Differences at low temperature can also arise from the partial alignment of crystallites in the rolling and annealing procedures. The precession experiments

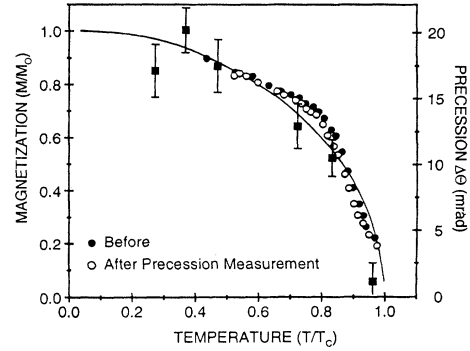


FIG. 1. Temperature dependence of the magnetization of thin gadolinium foil and measured precession  $\Delta\theta$  of the gamma-ray angular correlation for the  $2_1^+ \rightarrow 0_1^+$  transition in  $^{150}\text{Sm}$ . The solid and open circles correspond to measurements carried out before and after the precession measurements, respectively. The solid squares refer to the precession data normalized at  $T = 137$  K. The line represents the Brillouin function for gadolinium metal having total angular momentum  $J = 7/2$ .  $T_C$  is the Curie temperature for gadolinium.

were carried out with the targets mounted on the cryotip of a closed-cycle Displex refrigeration unit set to maintain a target temperature of 40 K and were maintained in an external polarizing field of 0.09 T.

Four Ge(Li) detectors with efficiencies ranging from 14% to 30% were placed at  $(\pm 63^\circ, \pm 117^\circ)$  or  $(\pm 67^\circ, \pm 113^\circ)$ . The gamma decay was measured in coincidence with beam ions backscattered into an annular silicon surface barrier detector (100  $\mu\text{m}$  depletion depth) which subtended a solid angle of  $165^\circ$ – $175^\circ$ . Signals from coincident gamma rays corresponding to the alternating direction of the external polarizing field (4 min field-flip cycle)

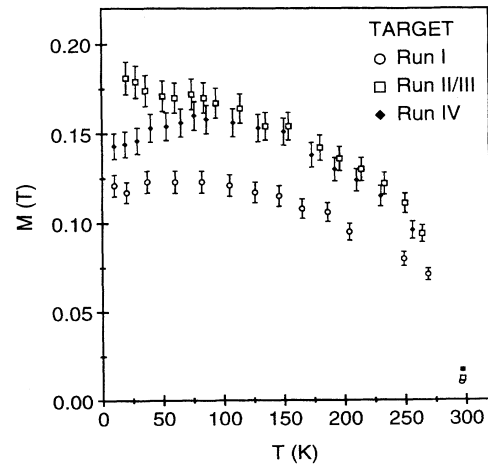


FIG. 2. Target magnetization as a function of temperature measured in a polarizing field of 0.09 T using an ac magnetometer. The error bars represent a  $\pm 5\%$  uncertainty in the measurements.

were routed appropriately.

Data were recorded in "event mode." All particle, gamma-ray, and corresponding time signals within 300 ns of a fast coincidence were recorded. Software windows set on appropriate backscattered particle energy and time spectra were applied to sort prompt and random coincident gamma spectra for each detector and field direction. At Rutgers, data were collected and analyzed on line. At Yale, data were collected on tape using the Oak Ridge data acquisition system and analyzed off line at Rutgers. The rotation  $\Delta\theta$  of the gamma-ray angular correlation was deduced from the double ratio of the coincident counting rates [20],

$$\rho_{ij} = \sqrt{\frac{N_i^\uparrow / N_i^\downarrow}{N_j^\uparrow / N_j^\downarrow}} \quad \text{and} \quad \rho = \sqrt{\frac{\rho_{14}}{\rho_{23}}}, \quad (1)$$

where the subscripts  $i = 1, 2$ ,  $j = 3, 4$  represent the four detectors.  $N \uparrow \downarrow_{(i,j)}$  is the random and background-subtracted coincidence counting rate in the photopeak of the  $i$ th and  $j$ th detector with the external field pointing up or down with respect to the plane of the reaction. The measured effect  $\epsilon = (\rho - 1)/(\rho + 1)$  is related to the rotation  $\Delta\theta$  and the logarithmic slope  $S$  of the angular distribution at the angle where the measurement is taken by  $\epsilon = S\Delta\theta$ . Corresponding cross ratios were monitored and found to be unity, ensuring that no systematic asymmetries perturb the results. Typical particle and gamma-ray coincidence spectra are shown in Figs. 3 and 4.

The unperturbed particle-gamma angular distribution  $W(\theta)$  for the  $2_1^+ \rightarrow 0_1^+$  gamma rays was measured for a target of  $0.493 \text{ mg/cm}^2$  Pt electroplated onto a thick copper backing. To minimize absorption effects from the cryogenic target mount, the target was mounted on a standard pole piece. Gamma-ray yields from the three Pt isotopes were combined and fit to a Legendre polynomial function with substate population fractions appropriate to the transition and gamma-ray detector ge-

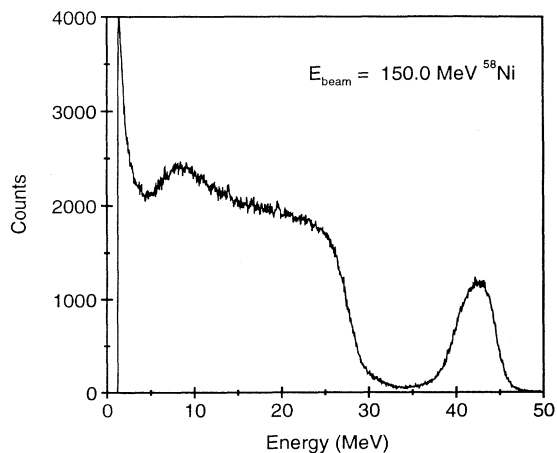


FIG. 3. Coincidence spectrum of nickel ions backscattered from the target of run III.

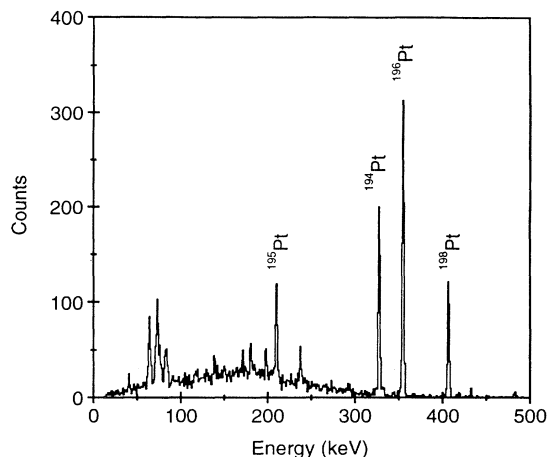


FIG. 4. Gamma-ray spectrum in coincidence with particles backscattered from a Pt target.

ometry as free parameters. The  $2_1^+ \rightarrow 0_1^+$  angular correlation is shown in Fig. 5. The values of the slope,  $S = (1/W)(dW/d\theta)$ , of the angular distribution at the detector angles above were then determined. In addition, the angular distribution and slope for each target were experimentally verified to match that of Fig. 5.

### III. RESULTS

#### A. $g$ factors

Experimentally determined values for the slope  $S$  of the gamma-ray angular correlation and the angular precession  $\Delta\theta$  are shown in Table II. The calculated ratio of the Pt precessions of  $^{194,196,198}\text{Pt}$  to  $\Delta\theta(^{194}\text{Pt})$  are also shown in Table II and are plotted in Fig. 6 with the average ratio of  $\Delta\theta(^{196,198}\text{Pt})$  for each run. Values for the Pt  $g$  factors normalized to  $g(^{194}\text{Pt}) = 0.302(16)$  as well as a comparison to previous results are shown in Table

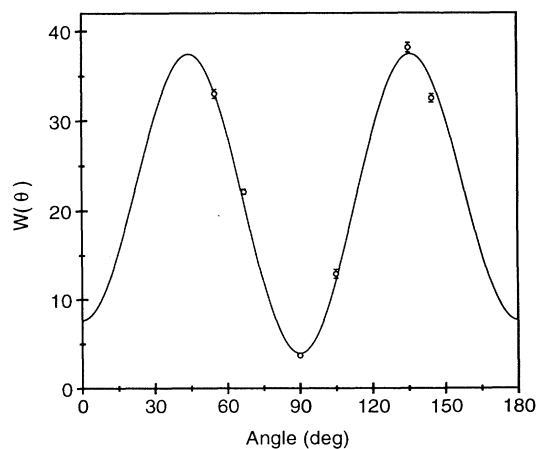


FIG. 5. Measured particle-gamma angular correlation for the  $2_1^+ \rightarrow 0_1^+$  transitions in  $^{194,196,198}\text{Pt}$ .

TABLE II. Summary of the angles at which the particle-gamma angular correlations were measured for each run and experimental results for the slopes of these angular correlations,  $S(\theta) = (1/W)(dW/d\theta)$ , the net precession angles  $\Delta\theta$ , and the ratio of the Pt precession to that of  $^{194}\text{Pt}$ .

Run Beam	$\theta_\gamma$ (deg)	$S(\theta)$ (rad $^{-1}$ )	Isotope	$\Delta\theta$ (mrad)	$\frac{\Delta\theta(^A\text{Pt})}{\Delta\theta(^{194}\text{Pt})}$
I 77 MeV $^{32}\text{S}$	$\pm 63$ $\pm 117$	2.491(7)	$^{194}\text{Pt}$	18.55(161)	1.00(12)
			$^{196}\text{Pt}$	15.46(149)	0.83(11)
			$^{198}\text{Pt}$	17.70(277)	0.95(17)
			$^{148}\text{Nd}$	11.32(128)	
II 80 MeV $^{32}\text{S}$	$\pm 67$ $\pm 113$	3.387(26)	$^{194}\text{Pt}$	24.55(189)	1.00(11)
			$^{196}\text{Pt}$	25.92(149)	1.06(10)
			$^{198}\text{Pt}$	27.72(233)	1.13(13)
III 150 MeV $^{58}\text{Ni}$	$\pm 67$ $\pm 113$	3.387(26)	$^{194}\text{Pt}$	16.48(157)	1.00(13)
			$^{196}\text{Pt}$	16.54(130)	1.00(12)
			$^{198}\text{Pt}$	18.46(195)	1.12(16)
IV 150 MeV $^{58}\text{Ni}$	$\pm 63$ $\pm 117$	2.491(7)	$^{194}\text{Pt}$	25.28(248)	1.00(14)
			$^{196}\text{Pt}$	29.74(203)	1.18(14)
			$^{198}\text{Pt}$	38.70(309)	1.53(19)
			$^{148}\text{Nd}$	16.00(175)	

III. With the exception of the results of Ref. [8], these data are in good agreement with prior measurements, but indicate a slightly larger  $g$  factor for  $^{198}\text{Pt}$  over that of  $^{194,196}\text{Pt}$ . The  $g$  factors reported in Ref. [8] for Pt recoiling in iron were deduced through the application of the Rutgers parametrization which does not account for the reported anomaly in the transient field at Pt nuclei in iron. However, as will be discussed below, this

anomaly in the transient field does not occur for Pt ions traversing gadolinium foils. The implications of the measurements of the  $g(2_1^+)$  factors on the nuclear structure of  $A \sim 190$  nuclei has been discussed extensively by Stuchbery, Lampard, and Bolotin [14] within the context of the interacting boson model IBM-2. While the  $g$  factors reported in Ref. [14] for  $^{194,196,198}\text{Pt}$  are nearly constant, the results of our work agree more closely with the overall systematics for Os and W where  $g$  increases with neutron number.

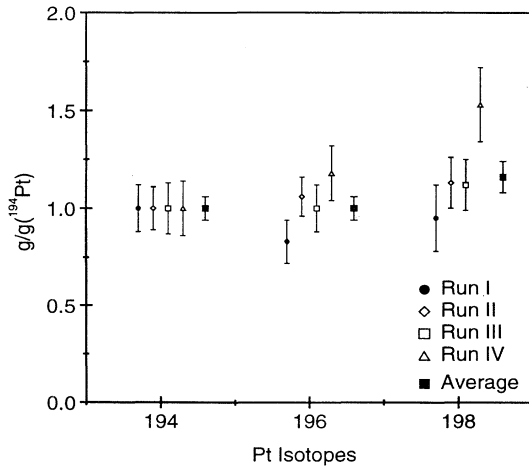


FIG. 6. Ratios of the Pt  $g$  factors to  $g(^{194}\text{Pt})$  as calculated from the measured angular precessions for each run. The average value for each isotope is represented by the solid squares.

### B. Transient field parametrization

In order to study the magnitude of the transient field acting at the recoiling ions in gadolinium, the average value of the field  $\langle B_{\text{TF}} \rangle$  was calculated from

$$\langle \dot{B}_{\text{TF}} \rangle = \frac{\Delta\theta}{\frac{\mu_N}{\hbar} g_{\text{expt}} \langle T \rangle}, \quad (2)$$

where  $\langle T \rangle$  is the average transit time of the ions in the gadolinium. For each Pt isotope,  $g_{\text{expt}}$  was taken to be the experimental value shown in Table III. For  $^{148}\text{Nd}$ , the weighted average of five values given in Ref. [32],  $g_{\text{expt}} = 0.355(12)$ , was used.  $\langle B_{\text{TF}} \rangle$  values for each Pt isotope and for  $^{148}\text{Nd}$  are shown in Table IV. For Pt, the mean values of  $\langle B_{\text{TF}} \rangle$  for  $^{194,196,198}\text{Pt}$  for each run are also shown.

A comparison was made to the Rutgers and Chalk River parametrizations of the transient field. The Rutgers parametrization [6, 23],

$$B_{\text{TF}} = (96.7 \pm 1.6) \left( \frac{v}{v_0} \right)^{0.45 \pm 0.18} Z^{1.1 \pm 0.2} M, \quad (3)$$

where  $M = \mu_B N_p$  ( $\mu_B$  is the Bohr magneton and  $N_p$  the volume density of polarized electrons in the ferromagnet) represents the measured target magnetization in Tesla, has been previously obtained as an overall fit for precession data for  $^{20}\text{Ne}$ ,  $^{24}\text{Mg}$ ,  $^{28}\text{Si}$ ,  $^{56}\text{Fe}$ ,  $^{82}\text{Se}$ ,  $^{106}\text{Pd}$ ,  $^{110}\text{Cd}$ ,  $^{134}\text{Ba}$ , and  $^{148}\text{Nd}$  nuclei recoiling through iron, and for  $^{82}\text{Se}$  and  $^{150}\text{Sm}$  recoiling through gadolinium in the velocity range  $1.9 \leq (v/v_0) \leq 6$ .

The Chalk River parametrization [11, 33],

$$B_{\text{TF}} = (27.5 \pm 1.0) \left( \frac{v}{v_0} \right) Z e^{-0.135(\frac{v}{v_0})} \quad (4)$$

was obtained for  $^{160}\text{Gd}$ ,  $^{164}\text{Dy}$ ,  $^{169}\text{Tm}$ , and  $^{207}\text{Pb}$ , recoiling in gadolinium for  $2.4 \leq (v/v_0) \leq 10.2$ . The amplitude of the field, 27.5, was obtained for a magnetization of  $6.3\mu_B/\text{atom}$  or 0.1778 T. In order to make this particular parametrization usable for foils with different magnetizations, Eq. (4) was rewritten in terms of  $M$  as

$$B_{\text{TF}} = (154.7 \pm 5.6) \left( \frac{v}{v_0} \right) Z e^{-0.135(\frac{v}{v_0})} M, \quad (5)$$

where  $154.7 \times 0.1778$  is equal to 27.5. The consistency of the current data with these two transient field calibrations is illustrated in Figs. 7 and 8. Included in these figures are  $B_{\text{TF}}$  values from the precession data for the first  $\frac{5}{2}^-$  state in  $^{207}\text{Pb}$  from Ref. [11], recalculated with the latest  $g$  factor  $g(\frac{5}{2}^-) = 0.30(1)$  [19]. Other data in this reference, for which the moments were not previously measured by an unambiguous technique, were omitted from the graphs. Additional data from published work in which target magnetizations are not reported in the papers were omitted as well. The data indicate a better agreement with the Rutgers than with the Chalk River parametrization. The Chalk River curve appears to overpredict the strength of the transient field by approximately 20% relative to the Rutgers parametrization. However, several of the  $g$  factors in Ref. [11] upon which the parametrization was based were inferred from nuclear physics systematics rather than precisely measured.

In addition, examination of the precessions obtained with  $^{32}\text{S}$  and  $^{58}\text{Ni}$  beams at the energies used in these experiments yields no indication of the beam-induced effects proposed by Speidel *et al.* [12, 13].

As previously stated, the experiments reported here were performed in four runs with three different targets.

TABLE III. Experimental average precession angle ratios and  $g$  factors for the  $2_1^+$  states in  $^{194,196,198}\text{Pt}$  with comparison to previous results.

Isotope Mean life (ps)	$\left\langle \frac{\Delta\theta(I)}{\Delta\theta(^{194}\text{Pt})} \right\rangle$	$g_{\text{expt}}$	Previous results <sup>b</sup>	Method
$^{194}\text{Pt}$ 60.3(9) <sup>c</sup> 59.7(22) <sup>e</sup>	0.302(16) <sup>a</sup>	0.302(16) <sup>a</sup>	0.296(22)	TF [14]
			0.295(10)	TF [15]
			0.203(6)	TF [8]
			0.292(17)	IMPAC [27] <sup>d</sup>
			0.26(3)	IMPAC [28]
			0.302(16)	radioactivity [18]
			0.254(13)	radioactivity [29]
$^{196}\text{Pt}$ 47.2(9) <sup>e</sup>	1.00(6)	0.302(24)	0.294(23)	TF [14]
			0.295(10)	TF [15]
			0.213(21)	TF [8]
			0.317(29)	TF [11] <sup>a</sup>
			0.297(33)	IMPAC [27] <sup>d</sup>
			0.28(2)	IMPAC [28]
			0.291(16)	radioactivity [29]
0.338(14)	radioactivity [30]			
$^{198}\text{Pt}$ 32.10(22) <sup>f</sup>	1.16(8)	0.350(30)	0.293(34)	TF [14]
			0.292(25)	TF [31] <sup>g</sup>
			0.308(48)	TF [11] <sup>a</sup>
			0.28(5)	IMPAC [28]

<sup>a</sup>Calculated relative to the adopted value  $g(^{194}\text{Pt}) = 0.302(16)$  of Katayama, Morinobu, and Ikegama [18] recalculated for mean life  $\tau=59.7(22)$  ps by Raghavan [19].

<sup>b</sup>IMPAC and radioactivity results reevaluated in Reference [14].

<sup>c</sup>Reference [25].

<sup>d</sup>Weighted average of measurements for Fe and Co hosts.

<sup>e</sup>Reference [19].

<sup>f</sup>Reference [26].

<sup>g</sup> $g$  factor relative to  $^{196}\text{Pt}$  recalculated in Ref. [14].

TABLE IV. Average transient field ( $B_{TF}$ ), calculated in Tesla from experimental  $g$  factors and angular precessions.  $\langle v/v_0 \rangle$  is the average of the entrance and exit velocities for the excited ions in the gadolinium layer.  $\langle T \rangle$  is the average transit time in picoseconds of the ions through the gadolinium, and  $M$  is the target magnetization in tesla measured at 40 K.  $\langle B_{TF} \rangle / M$  is the mean value of  $\langle B_{TF} \rangle$  for  $^{194,196,198}\text{Pt}$  and Nd divided by the measured bulk magnetization.

Run Beam	$\langle v/v_0 \rangle$	$\langle T \rangle$ (ps)	$M$ (T)	Isotope	$\langle B_{TF} \rangle$ (T)	$\frac{\langle B_{TF} \rangle}{M}$
I 77 MeV $^{32}\text{S}$	$2.27 \pm 0.36$	0.509	0.1230	$^{194}\text{Pt}$	2519(256)	18431(1333)
				$^{196}\text{Pt}$	2100(262)	
$^{198}\text{Pt}$	2074(370)					
	$2.70 \pm 0.50$	0.428		$^{148}\text{Nd}$	1555(184)	12642(1496)
II 80 MeV $^{32}\text{S}$	$2.32 \pm 0.44$	0.586	0.1770	$^{194}\text{Pt}$	2896(271)	16644(977)
				$^{196}\text{Pt}$	3058(300)	
				$^{198}\text{Pt}$	2882(339)	
III 150 MeV $^{58}\text{Ni}$	$4.04 \pm 0.54$	0.332	0.1770	$^{194}\text{Pt}$	3431(374)	19243(1299)
				$^{196}\text{Pt}$	3444(385)	
				$^{198}\text{Pt}$	3316(451)	
IV 150 MeV $^{58}\text{Ni}$	$3.72 \pm 0.80$	0.513	0.1580	$^{194}\text{Pt}$	3406(380)	25063(1570)
				$^{196}\text{Pt}$	4008(420)	
				$^{198}\text{Pt}$	4500(527)	
	$4.54 \pm 0.90$	0.417		$^{148}\text{Nd}$	2256(258)	14278(1633)

A comparison of the four runs shows that the relative measurements indicated by the precession ratios are in good agreement with each other, while there is a distinct scatter in the observed average transient field at similar ion velocities in different targets. The 15% spread in the data shown in Figs. 7 and 8 has been consistently observed in such experiments [6]. This scatter probably

reflects the difficulty in preparing the multilayer targets and evaluating the thickness and uniformity of each layer.

These observations further stress the point that precision magnetic moment measurements should not rely on the parametrizations chosen, but require comparisons with the data from states with known moments, in a same or neighboring element and in the same velocity range.

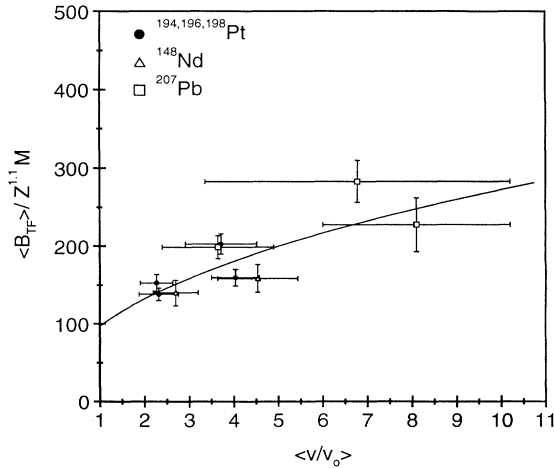


FIG. 7. Rutgers parametrization of the transient field plotted with the average transient field at Pt and Nd in gadolinium deduced from the precession data and at Pb in gadolinium from Ref. [11].

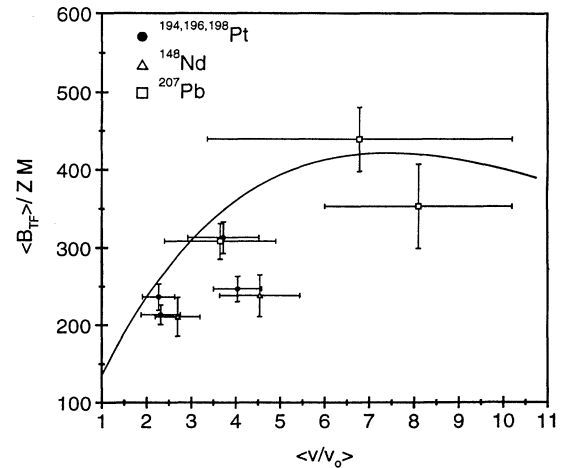


FIG. 8. Chalk River parametrization of the transient field plotted with the average transient field at Pt and Nd in gadolinium deduced from the precession data and at Pb in gadolinium from Ref. [11].

#### IV. CONCLUSIONS

Angular precessions for  $^{194,196,198}\text{Pt}$  and  $^{148}\text{Nd}$  recoiling through magnetized gadolinium have been measured and the magnetic moments of  $^{196,198}\text{Pt}$  relative to  $^{194}\text{Pt}$  obtained. These  $g$  factors are in good agreement with the measurements of the Australian and Padova groups and support the contention of an anomalously low transient field for Pt in iron. The magnitudes of the average transient field acting at  $^{194,196,198}\text{Pt}$  and  $^{148}\text{Nd}$  in gadolinium in the recoil velocity range  $1.9 \leq (v/v_0) \leq 4.6$  have been extracted from the angular precessions and combined with results for  $^{207}\text{Pb}$ . The data agree with the Rutgers calibration of the field. It should be noted that the transient field strength is strongly dependent

on the bulk magnetization of the target. In the case of gadolinium in which well magnetized foils are difficult to fabricate, a good measurement of target magnetization is essential for consistent measurements.

#### ACKNOWLEDGMENTS

We wish to thank A. Lipski and R. Klein for their assistance in target preparation and Dr. D. Barker, Dr. C. S. Lee, L. Farris, and R. Henry for their help in running the experiments. We also acknowledge the help and support of the students and technical staff of the Wright Nuclear Structure Laboratory. This work was supported in part by the National Science Foundation.

- 
- [1] R. R. Borchers, J. D. Bronson, D. E. Murnick, and L. Grodzins, *Phys. Rev. Lett.* **17**, 1099 (1966).
  - [2] R. R. Borchers, B. Herskind, J. D. Bronson, L. Grodzins, R. Kalish, and D. E. Murnick, *Phys. Rev. Lett.* **20**, 424 (1975).
  - [3] J. L. Eberhardt, G. van Middelkoop, R. E. Horstman, and H. A. Doubt, *Phys. Lett.* **56B**, 329 (1975).
  - [4] J. Lindhard and A. Winther, *Nucl. Phys.* **A166**, 413 (1971).
  - [5] J. L. Eberhardt, R. E. Horstman, P. C. Zalm, H. A. Doubt, and G. van Middelkoop, *Hyperfine Interact.* **3**, 195 (1977).
  - [6] N. K. B. Shu, D. Melnik, J. M. Brennan, W. Semmler, and N. Benczer-Koller, *Phys. Rev. C* **21**, 1828 (1980).
  - [7] H. R. Andrews, O. Häusser, D. Ward, P. Taras, R. Nicole, J. Keinonen, P. Skensved, and B. Haas, *Nucl. Phys.* **A383**, 509 (1982).
  - [8] R. Levy, N. Tsoupas, N. K. B. Shu, A. Lopez-Garcia, W. Andrejtscheff, and N. Benczer-Koller, *Phys. Rev. C* **25**, 293 (1982).
  - [9] A. E. Stuchbery, C. G. Ryan, and H. H. Bolotin, *Hyperfine Interact.* **13**, 275 (1983).
  - [10] D. Bazzacco, F. Brandolini, K. Loewenich, P. Pavan, C. Rossi-Alvarez, R. Zammoni, and M. De Poli, *Phys. Rev. C* **33**, 1785 (1986).
  - [11] O. Häusser, H. R. Andrews, D. Horn, M. A. Lone, P. Taras, P. Skensved, R. M. Diamond, M. A. Deleplanque, E. L. Dines, A. A. Machiavelli, and F. S. Stephens, *Nucl. Phys.* **A412**, 141 (1984).
  - [12] K.-H. Speidel, M. Knopp, W. Karle, M.-L. Dong, J. Cub, U. Reuter, H.-J. Simonis, P. N. Tandon, and J. Gerber, *Phys. Lett. B* **227**, 16 (1989).
  - [13] K.-H. Speidel, U. Reuter, J. Cub, W. Karle, F. Passek, H. Busch, S. Kremeyer, and J. Gerber, *Z. Phys. D* **22**, 371 (1991).
  - [14] A. E. Stuchbery, G. J. Lampard, and H. H. Bolotin, *Nucl. Phys.* **A528**, 447 (1991).
  - [15] F. Brandolini, M. Ionescu-Bujor, P. Pavan, D. Bazzacco, C. Rossi-Alvarez, M. De Poli, A. M. Haque, and R. V. Ribas, *Nucl. Phys.* **A536**, 366 (1992).
  - [16] E. Bodenstedt, B. Hamer, P. Herzog, J. van den Hoff, H. Munning, S. Piel, J. Prinz, and R. Sajok, *Z. Phys. A* **342**, 249 (1992).
  - [17] M. Kontani and J. Itoh, *J. Phys. Soc. Jpn.* **22**, 345 (1967).
  - [18] I. Katayama, S. Morinobu, and H. Ikegami, *Hyperfine Interact.* **1**, 113 (1975).
  - [19] P. Raghavan, *At. Data Nucl. Data Tables* **42**, 189 (1989).
  - [20] N. Benczer-Koller, M. Hass, and J. Sak, *Annu. Rev. Nucl. Part. Sci.* **30**, 53 (1980).
  - [21] N. Benczer-Koller, *Hyperfine Interact.* **24-26**, 461 (1985).
  - [22] J. F. Ziegler, *Appl. Phys. Lett.* **31**, 544 (1977).
  - [23] N. Benczer-Koller, D. J. Ballon, and A. Pakou, *Hyperfine Interact.* **33**, 37 (1987).
  - [24] A. Piqué, J. M. Brennan, R. Darling, R. Tanczyn, D. Ballon, and N. Benczer-Koller, *Nucl. Instrum. Methods A* **279**, 579 (1989).
  - [25] B. Singh, *Nucl. Data Sheets* **56**, 75 (1989).
  - [26] Zhou Chunmei, *Nucl. Data Sheets* **60**, 527 (1990).
  - [27] D. A. Garber, M. Behar, Z. W. Grabowski, and Wm. C. King, *Z. Phys.* **270**, 163 (1974).
  - [28] R. Kalish, L. Grodzins, R. R. Borchers, J. D. Bronson, and B. Herskind, *Phys. Rev.* **161**, 1196 (1967).
  - [29] I. Berkes, R. Rougny, M. Meyer-Lévy, R. Chéry, J. Danière, G. Lhersonneau, and A. Troncy, *Phys. Rev. C* **6**, 1098 (1972).
  - [30] M. Kawamura, T. Tomiyama, and H. Kato, *J. Phys. Soc. Jpn.* **50**, 1832 (1981).
  - [31] A. E. Stuchbery, C. G. Ryan, H. H. Bolotin, I. Morrison, and S. H. Sie, *Nucl. Phys.* **A365**, 317 (1981).
  - [32] A. E. Stuchbery, G. J. Lampard, and H. H. Bolotin, *Nucl. Phys.* **A516**, 119 (1990).
  - [33] O. Häusser, H. R. Andrews, D. Ward, N. Rud, P. Taras, R. Nicole, J. Keinonen, P. Skensved, and C. V. Stager, *Nucl. Phys.* **A406**, 339 (1983).